Journal of Electroanalytical Chemistry 618 (2008) 11–16

Contents lists available at ScienceDirect

Journal of Electroanalytical Chemistry

journal homepage: www.elsevier.com/locate/jelechem

# Electrodeposition of gold on tungsten nanowires present in NiAl–W eutectics

Belen Bello Rodriguez, Andrew Jonathan Smith, Achim Walter Hassel *

*Max-Planck-Institut für Eisenforschung GmbH, Max-Planck-Strasse 1, 40237 Düsseldorf, Germany*

ARTICLE INFO

*Article history:*
Received 5 August 2007
Received in revised form 19 February 2008
Accepted 20 February 2008
Available online 5 March 2008

*Keywords:*
Nanopores
Electrodeposition
Nucleation and growth
Nanoelectrode array

ABSTRACT

The formation of gold nanoelectrode arrays was investigated by electrodeposition of the metal on the tungsten nanowires present in directionally solidified NiAl–W eutectics. The tungsten fibres present in the eutectic were conditioned prior to the electrodeposition, and the NiAl matrix was simultaneously passivated by formation of $Al_2O_3$ oxide. The simultaneous oxidation of W to W(VI) species for the formation of nanopores, and growth of passive $Al_2O_3$ oxides on the NiAl matrix was studied for different polarisation potentials. Anodisation of the samples at potentials <0.7 V resulted in the formation of thin oxide films, and therefore the NiAl matrix remained partially active. In order for the matrix to be fully passive, and the fibres to dissolve and form nanopores, the initial polarisation must be run at 0.7 V vs. SHE. The electrodeposition of gold on the conditioned samples was afterwards optimised for the filling of the pores. When the deposition was run by application of reverse current pulses the obtained gold structures presented a hemispherical shape with a radius that increased with the duration of the cathodic pulse. The electrodeposition of gold from more diluted Au(I) solutions under potentiostatic conditions yielded the formation of thin Au deposits in the nanopores. The nucleation and growth mechanisms involved in the process were determined from the potentiostatic current transients in all the examined cases. It was found that instantaneous nucleation took place for the more concentrated solutions, whereas mixed processes were observed for diluted amounts of Au(I).



## 1. Introduction

The growth of pores in metals and semiconductors by electrochemical techniques has been studied since the 1950s [1], and this approach has been the subject of much interest in recent years because of its suitability for the formation of ordered-nanostructures. The most common substrate employed for the template-assisted deposition of nanostructures in pores is anodised alumina [2–5]. However, despite the many advantages that such a template presents, it often requires severe chemical or physical treatments for the formation of the pores and their conditioning prior to the electrodeposition process. On the contrary, a simpler method to exploit the excellent stability and passive properties of $Al_2O_3$ has recently been introduced. The use of pseudo-binary eutectic alloys composed of a NiAl matrix and Re/W as minor phase has proved a suitable alternative protocol for the formation of ordered pore arrays [6]. The use of such systems as substrate for the electrodeposition of ordered structures is of considerable interest, since all Re and W can be grown as well-aligned nanofibres in the NiAl matrix. The matrix is passivated by formation of $Al_2O_3$ oxide, with the simultaneous oxidation of the fibres to create nanopores. These pores are well ordered and aligned, and are excellent substrates for the formation of nanostructure arrays [6–8]. The use of Re/W also exhibits the advantage that the oxides of both metals have metallic or semiconducting characters [9,10], and therefore any oxide growth on the fibres will only affect minimally their electrochemical activity. The suitability of a NiAl–Re eutectic as a template for the formation of gold hemispheres by electrodeposition has already been studied [11,12]. The experimental conditions required for the electrodeposition of gold into the pores have been optimised for the formation of gold sensor arrays with an average diameter of ~400 nm [12]. In the current work, the use of the alternative system NiAl–W as a substrate for electrodeposition is investigated. The advantages of this system when compared to Re containing eutectics is the smaller size of the W fibres (100–200 nm) for a sample processed under the same conditions, which would reduce the size of the deposited structure. The interfibrous spacing is also larger than in the NiAl–Re system, and thus overlapping of the diffusion layers of each nanoelectrode can be reduced. The work described here reports on investigations carried out on the electrodeposition of gold into the nanopores formed in a NiAl–W eutectic. The pores are initially created by polarisation of the sample at the optimal conditions for the simultaneous dissolution of the fibres and the passivation of the NiAl matrix. The kinetics of the gold deposition was then investigated by application of reverse and constant potential pulses. In summary, it is possible to select the optimal conditions for the selective deposition of gold into

* Corresponding author. Fax: +49 211 6792 218.
*E-mail address:* hassel@elchem.de (A.W. Hassel).

0022-0728/$ - see front matter © 2008 Elsevier B.V. All rights reserved.
doi:10.1016/j.jelechem.2008.02.021

the pores, with the formation of arrays of gold nanosensors. Such arrays may find applications as analytical tools in various fields.

## 2. Materials and methods

### 2.1. Eutectic solidification

NiAl–W eutectics were solidified according to a protocol described previously [6]. As a starting material, nickel (99.97 wt.%), electrolytic aluminium (99.9999 wt.%) and tungsten pellets (99.9 wt.%) were used for the alloy preparation. The directional solidification was conducted at a temperature of 1690 ± 10 °C, a thermal gradient of approximately 40 K $cm^{-1}$ and a growth rate of 8.3 μm $s^{-1}$. The microstructure of the obtained unidirectionally solidified NiAl–W eutectic exhibited fully eutectic morphology consisting of a cell structure with a mean cell diameter of 500 μm and a length covering the entire length of the rod-like sample. A diameter of 200 nm was found for the tungsten wires, and the mean inter fibre spacing was 3 μm. The fibre orientation was (100) referring to the rod axis of the directionally solidified sample.

### 2.2. NiAl–W passivation

The electrochemical passivation of the NiAl matrix was carried out by polarisation of the eutectic alloy in 1 M acetate buffer (pH 6.0). A conventional three-compartment cell (approx. volume 50 mL) with working, reference and counter electrodes was employed in all experiments. The samples were mechanically mirror-like grinded and polished prior to the measurements. A commercial Ag/AgCl electrode was used as reference (Metrohm, Filderstadt, Germany). A smooth Au foil electrode was employed as counter (apparent surface area = 2 $cm^2$). A PST050 potentiostat (Radiometer Analytical, Lyon, France) was used in all electrochemical measurements. Measurements were performed at room temperature in quiescent solutions. All potentials are given vs. the standard hydrogen electrode (SHE).

### 2.3. Gold electrodeposition

The electrodeposition of gold was carried out from a commercial bath containing 12 g $L^{-1}$ of gold sulfite (in the form of $(NH_4)_3Au(SO_3)_2$) in neutral pH (Metakem, Usingen, Germany) [13]. For the studies on the evolution of the deposits with deposition time and potential, the plating was carried out by application of rectangular reverse pulses [14]. The potential was switched from −0.7 V to 0.1 V (against anode) at a ratio of 1:10 s. The duration of the cathodic pulse was varied from 1 ms to 3 s, and the concentration of Au(I) was kept constant at 76 mM. The studies on the nucleation and growth of the gold deposits were carried out by running potentiostatic measurements at −0.7 V (vs. counter) and examining the recorded current transients. These experiments were performed with different concentrations of Au(I) (1.5 mM–76 mM), after appropriate dilution of the plating bath in 0.1 M $Na_2SO_4$. All experiments were performed at room temperature in non deaerated solutions.

Cyclic voltammetric analyses of the $(NH_4)_3Au(SO_3)_2$ plating bath were carried out in a three-compartment electrochemical cell, with a gold counter electrode (apparent area = 2 $cm^2$), a Ag/AgCl reference electrode (connected to the cell by a Luggin capillary), and a tungsten wire as working electrode (diameter = 1 mm). The scans were started at OCP (−55 mV vs. SHE), then progressed in a cathodic direction to −0.8 V, anodically to 1.2 V (vs. SHE), and then back to OCP. The scan rate was 10 mV $s^{-1}$. The plating solution was diluted 10-fold to a final concentration of 3.8 mM in $Na_2SO_4$. Identical scans were run for a solution containing $Na_2SO_3$ (also diluted in $Na_2SO_4$) as a blank.

### 2.4. Scanning electron microscopy

Scanning electron microscopy pictures were obtained using a Leo 1550 VP apparatus (Leo Elektronenmikroskopie GmbH, Oberkochen, Germany) fitted with an INCA Energy Dispersive System (EDS) (Oxford Instruments, Oxford, UK).

All materials used were of analytical grade and purchased by Merck (Darmstadt, Germany).

## 3. Results and discussion

### 3.1. Effect of the passivation potential on the electrodeposition of gold

Initial experiments looked at the effect of the passivation pre-treatment on the consequent electrodeposition. Gold will be selectively deposited on the tungsten fibres if the NiAl matrix is previously passivated by formation of at least one of the oxides $Al_2O_3$ or NiO. Ideally, this initial passivation should not affect the tungsten fibres, so that their electrochemical activity is not compromised during the deposition process. According to the *E–pH* diagram for each of the elements in the system (Ni, Al, W), $Al_2O_3$ is formed over a wide range of *E* and *pH*, and therefore passivation of the matrix by formation of this oxide should not present a problem (Fig. 1, adapted from Ref. 15). The immunity range of tungsten extends over a wide pH range (−2 to 14) for potentials below −0.4 V. However, it easily forms oxides of different nature at potentials above −0.2 V. If the passivation is run at a potential value at which W remains metallic (−0.6 V), the formed aluminium oxide is very thin and with a large number of defects [12]. Also, nickel may stay in the metallic state under those conditions. As a consequence, the passive oxide layer is very brittle and susceptible to corrosion. The subsequent electrodeposition takes place not only on the tungsten fibres, but also in the defects present in the NiAl matrix, thus yielding inhomogeneous gold structures randomly distributed on the whole surface.

The formation of gold microelectrode arrays depends on the selective deposition of the metal on the fibres [11]. Dissolution of the fibres to create nanopores enables the formation of aligned gold nanoelectrodes, with the dimensions of the pores into which they were grown [12]. According to the *E–pH* diagram for W, Ni, and Al [15], a polarisation at potentials above 0 V would yield the formation of passive $Al_2O_3$ and $Ni(OH)_2$ species on the surface of the alloy, with W being oxidized to soluble $WO_4^{2-}$ species. The effect of the applied anodic potential on the samples passivation

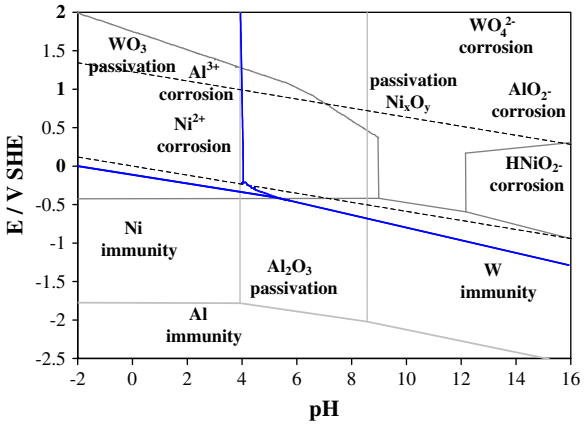


**Fig. 1.** Combined *E*–pH diagram for NiAl–W.

was examined by running potentiostatic scans for NiAl–W systems at 0.5 V and 0.7 V. The obtained current densities displayed a large initial value which decayed with time, with a decrease being slightly lower when the sample was exposed to 0.5 V (Fig. 2). The scan at this potential also showed a small shoulder during the initial polarisation times (approximately 50 s). The high initial current recorded, as well as the observed shoulder peak, may be attributed to the oxidation of tungsten from the alloy. The levelling off marks the transition of the reaction to a diffusion controlled process. The log ($i$) vs. log ($t$) plots presented a slope much smaller than $-1$ in both cases. The growth of the $Al_2O_3$ film on the surface of the matrix should follow the high field theory, and therefore the graphs were expected to have a $-1$ slope. This deviation from linearity may be a consequence of the simultaneous occurrence of a series of processes, namely growth of oxide film in equilibrium with corrosion of the film after a sufficiently long time, and oxidation of tungsten to various species [8].

The degree of passivity showed by the oxide film after the described polarisation processes was evaluated in terms of the amount of gold deposited on the NiAl matrix. The electrodeposition of gold on samples polarised at 0.5 V produced only a small number of gold nuclei on the NiAl matrix, suggesting that the anodic polarization yields a more perfect surface passivation than the polarisation run at cathodic potentials. However, a complete disappearance of gold structures on the NiAl matrix was only achieved after the pre-treatment at 0.7 V. A compact passive film which hinders electron transfer reactions necessary for the reduction of gold and the electrodeposition is achieved by polarisation of the samples at anodic potentials $\geqslant$0.7 V.

### 3.2. Studies on the evolution of the gold deposits with the duration of the electrodeposition process

The formation and growth of the gold structures on the W fibres was initially evaluated by examining the evolution of the gold deposits with the application of short pulses [12]. The increase in size of the gold deposits with the duration of the electrodeposition process (related to the total number of applied pulses) was deduced from the SEM pictures obtained for a given sample subjected to small number of pulses with a duration varying between 1 ms and 1 s. The deposition process was accomplished by application of short cathodic pulses (1 ms–1 s), followed by 10-times longer anodic pulses to allow diffusion of the ions from the bulk solution to the electrode/solution interface. The application of anodic pulses also allows for the surface to be cleaned of any impurity that would deposit on the fibres alongside the gold nuclei.

The evolution of the size of the gold deposits with the duration of the applied pulse is shown in Fig. 3. For cathodic pulses with a duration <50 ms it is necessary to apply a large number of consecutive pulses (~20–50) to observe significant gold deposits. If the cathodic pulses have a duration of 50 ms, gold structures of large diameter are observed after the application of only five consecutive pulses. The size of the spheres increases steadily with the amount of applied pulses (total applied charge increased). However, the diameter seems to be slightly smaller than expected for the application of 0.5 s pulses. These long pulses mean that a larger amount of charge is passed through the sample. Therefore, the nucleation process could be favoured, resulting in the formation of a larger number of gold deposits when compared to shorter pulses, but of smaller size. The density of observed gold spheres increases initially, but after the application of a sufficiently large charge it reaches a constant value due to the overlapping of growing spheres. Fig. 4 shows examples of the obtained gold spheres.

The fact that a large number of cycles is needed when the duration of the cathodic pulse is <50 ms indicates that not all the charge applied with each pulse is consumed in the electrodeposition. Part of the charge may be consumed in charging of $Al_2O_3$ and NiO oxides, and possible corrosion of any film of tungsten oxides on the fibres surface. However, it is worth noting that the observation of gold spheres takes place with the application of shorter pulses as well as total deposition time than when the used substrate is a NiAl–Re eutectic [12]. The possible oxidation of Re to form different oxides may be a drawback for its use as a reliable electrode. On the other hand, tungsten remains in the metallic state over a wider potential range [15], and its oxides are metallic or semiconducting, so that the sample resistance is not greatly affected. These properties may ensure that the efficiency of the electrodeposition process is greater with the use of W as a substrate electrode.

### 3.3. Investigations on the nucleation and growth of gold into W nanopores

The nucleation and growth of gold structures in the tungsten pores was determined from potentiostatic analyses of diluted Au(I) solutions. The potential at which the electrodeposition would be done was initially evaluated by cyclic voltammetry. The obtained cyclic voltammograms are shown in Fig. 5 for a 3.8 mM $(NH_4)_3Au(SO_3)_2$ solution. The voltammetry was started at OCP and scanned in the cathodic direction. The reduction scan is

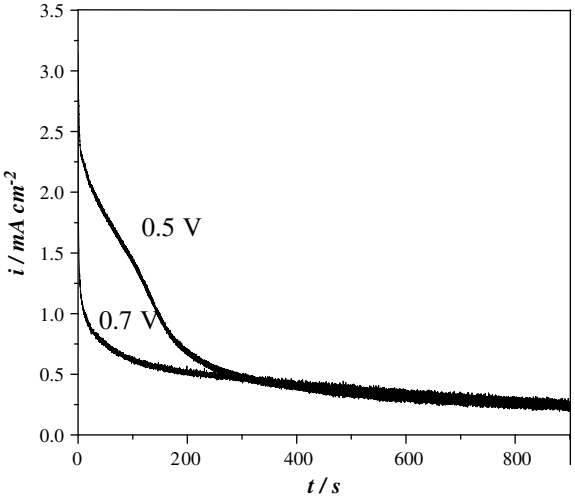


**Fig. 2.** Current transients recorded for the potentiostatic anodisation of NiAl–W samples at 0.5 V and 0.7 V vs. SHE.

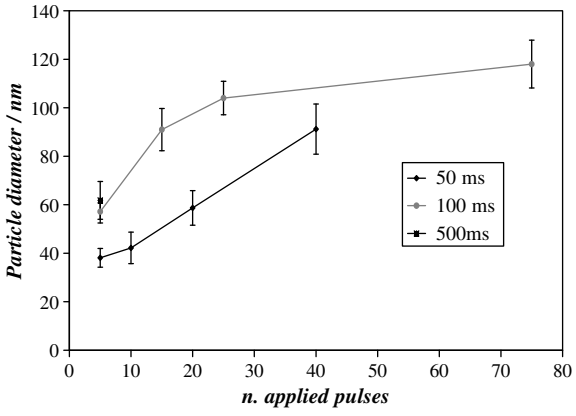


**Fig. 3.** Increase in the diameter of the deposited gold spheres with the duration of the electrodeposition process for the application of increasing numbers of short cathodic pulses.

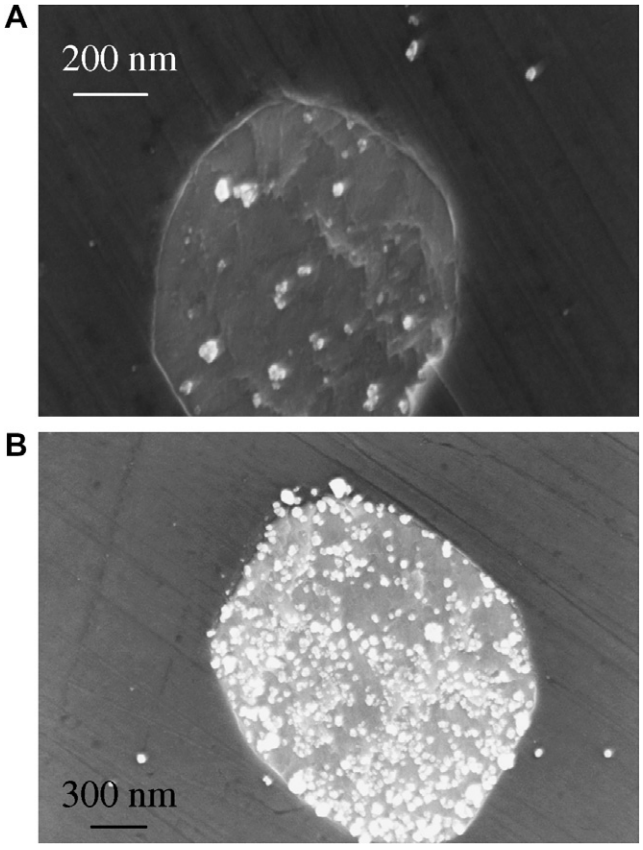


**Fig. 4.** Examples of gold deposits obtained on W fibres with the application of cathodic pulses of increasing duration (−0.7 V vs. anode), followed by a 10-fold longer anodic pulses (0.1 V vs. anode). (A) Cathodic pulses of 50 ms, total deposition time = 1 s; (B) cathodic pulses of 100 ms, total deposition time = 1.5 s.

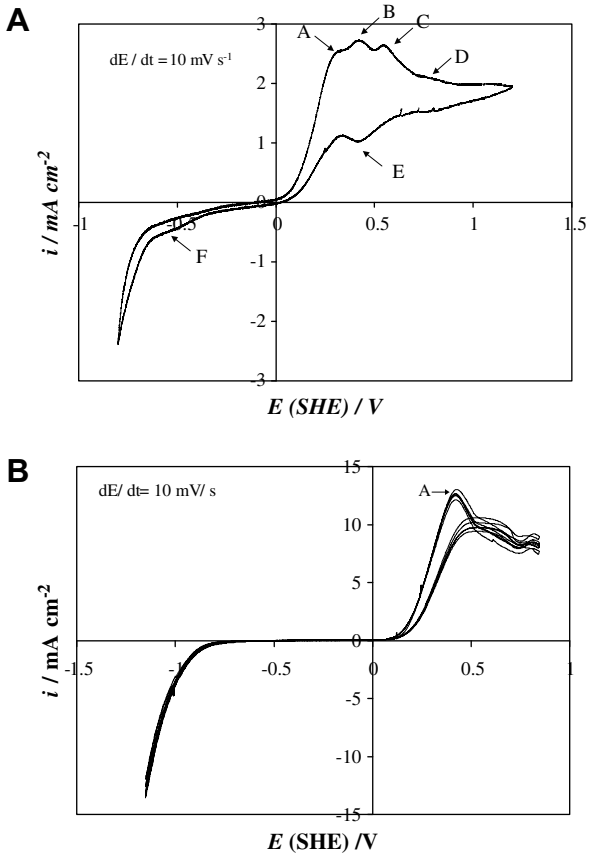


**Fig. 5.** Potentiodynamic scans recorded for (A) $(NH_4)_3Au(SO_3)_2$ in $Na_2SO_4$, and (B) $Na_2SO_3$ in $Na_2SO_4$ (blank). A W wire (diameter = 0.1 cm) was used as working electrode after passivation at 0.7 V vs. SHE for 15 min.

characterised by a large current peak at −0.62 V (peak F in Fig. 5), attributable to the reduction of Au(I) ions to Au(0) on the W wire. In the anodic scan, four peaks are observed, at 0.32 V, 0.44 V, 0.60 V and 0.79 V (peaks A–D in Fig. 5A). An additional reduction peak is observed in the following reverse scan at 0.36 V (peak E in Fig. 5A). Cyclic voltammograms recorded for a solution containing sulfite ions (without the presence of Au(I)) showed only one significant oxidation peak at 0.44 V, which correlates to peak B found on the Au(I) solution scans. This peak may therefore be attributed to the oxidation of the $SO_3^{2-}$ electrolyte to $SO_4^{2-}$. The additional peaks observed for the anodic scan in Fig. 5.A might be the results of the simultaneous occurrence of a series of reactions involving the oxidation Au(I) to Au(III), and the oxidation of the W electrode to W(VI) species through W(IV) and W(V) intermediates [16]. Thus, metallic W is expected to form $WO_2$ and $WO_3$ oxides before forming soluble $WO_4^{2-}$ ions, with the resulting increase in recorded current. Additionally, the $W_xO_y$ oxides may be reduced in consecutive cathodic scans, which would explain the appearance of a small current loop at −0.5 V in further cycles. The presence of additives in the bath may also play a role in the electrochemical behaviour of the solution, considering those additives are susceptible to oxidation and/or reduction. More experiments should be run to exactly identify each of the oxidation peaks. However, the work reported in this manuscript deals only with the optimisation of the conditions for the electrodeposition of gold into the pores, and the studied voltammogram gives enough information on that point regarding the necessary potential to apply for the reduction of Au(I) ions.

These results suggest that the electrodeposition of gold is feasible at potentials more cathodic than −0.62 V. Based on this finding, the electrodeposition of gold was subsequently investigated at −0.70 V (vs. anode). This potential was approximated to the one observed vs. SHE but taking into account the use of a two-electrode configuration.

The current transients obtained for the electrodeposition of gold at −0.70 V from different concentrations of the Au(I) salt are shown in Fig. 6. For each current transient, there is initially a charg-

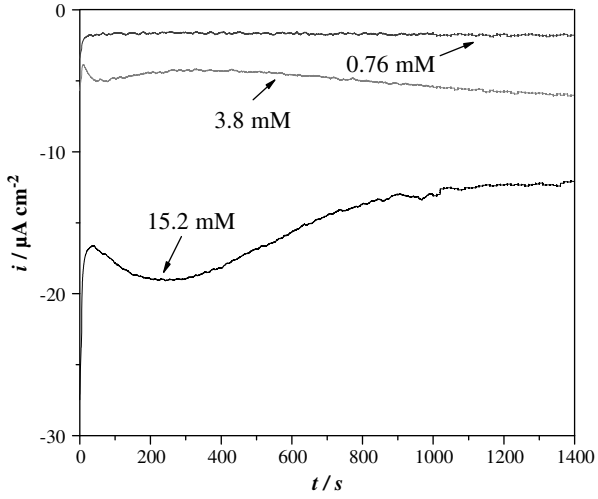


**Fig. 6.** Current transients recorded for the electrodeposition of Au on NiAl–W samples at −0.7 V (vs. counter) for different concentrations of Au(I) ions.

ing current that decays during the nucleation and growth processes. For a concentration of 15.2 mM Au(I) (black plot) the current density showed a sharp increase at short times, then reached a minimum negative value at $-16.6\ \mu A\ cm^{-2}$ ($i_{max}$) after ~39 s ($t_{max}$), then decreased abruptly and finally rose again to a value of $-12.4\ \mu A\ cm^{-2}$ (Fig. 6). For a solution containing 3.8 mM of Au(I), the current reaches its minimum negative value of $-3.9\ \mu A\ cm^{-2}$ ($i_{max}$) after ~13 s ($t_{max}$), and decreases afterwards to $-4.4\ \mu A\ cm^{-2}$ after ~500 s (light gray plot on Fig. 6). The current transient obtained in the presence of 0.76 mM Au(I) showed an initial increase in the current to a minimum negative value of $-1.82\ \mu A\ cm^{-2}$ after ~39 s. However, in contrast to previous examples, this value remains constant afterwards, suggesting that linear diffusion dominates the process (grey plot on Fig. 6). The decrease in cathodic current observed in all three cases reflects the increase in electroactive area due to either the growth of the nuclei in size, or the formation of more nuclei. The nuclei also develop their own diffusion zones, which overlap as they grow giving way to an overall linear mass transfer characteristic of a planar electrode. Consequently, the current falls as the transient approaches that of a linear diffusion for the total electrode surface [17]. When the current reaches the diffusion limited region, its behaviour can be described by the Cottrell equation:

$$i = \frac{zFD^{1/2}c}{\pi^{1/2}t^{1/2}} \quad (1)$$

The most accepted model to describe the nucleation and growth processes during electrodeposition defines two distinctive cases: instantaneous and progressive nucleation [17,18]. Instantaneous nucleation takes place when the number of formed nuclei reaches a constant value rapidly, whereas in progressive nucleation new nuclei are constantly formed. The process associated with the experimental results can be established from the plots depicting the reduced parameters $(i/i_{max})^2$ vs. $(t/t_{max})$, being $i_{max}$ and $t_{max}$ the minimum negative current, and the time at which it was reached, respectively. In the case of instantaneous nucleation, the relationship between $(i/i_{max})$ and $(t/t_{max})$ follows the expression:

$$(i/i_{max})^2 = 1.9542(t/t_{max})^{-1}(1 - \exp[-1.2564(t/t_{max})])^2 \quad (2)$$

When progressive nucleation takes place, that relationship is given by [17,18]:

$$(i/i_{max})^2 = 1.2254(t/t_{max})^{-1}(1 - \exp[-2.3367(t/t_{max})^2])^2 \quad (3)$$

In order to determine the process involved in the operating conditions used here the experimental data was converted to its reduced form ($i/i_{max}$ vs. $t/t_{max}$) and plotted along with the theoretical graph for comparison (Fig. 7). Under these experimental conditions, the electrochemical deposition of gold would be expected to follow an instantaneous nucleation, since the number of nuclei is limited to the density of tungsten fibres present on the structure. The experimental data obtained for a concentration of 15.2 mM Au(I) agreed well with the model described for an instantaneous nucleation. However, the reduced plot obtained for 3.8 mM Au(I) does not follow any of the suggested models accurately. For smaller Au(I) concentrations (0.76 mM) the current reached the diffusion zone soon after the deposition began, and thus it is better described by the Cottrell equation.

From the data obtained with 15.2 mM Au(I) it is possible to obtain information about the diffusion coefficient $D$ of the ion. $D$ is related to the product $(i_{max})^2 t_{max}$ according to:

$$(i_{max})^2 t_{max} = 0.1629(zFc)^2 D \quad (4)$$

where $F$ is the Faraday constant, $c$ the concentration of the ion, and $z$ the number of exchanged electrons. The value obtained from this relation for $D$ was $1.94 \times 10^{-7}\ cm^2\ s^{-1}$. This value is lower than

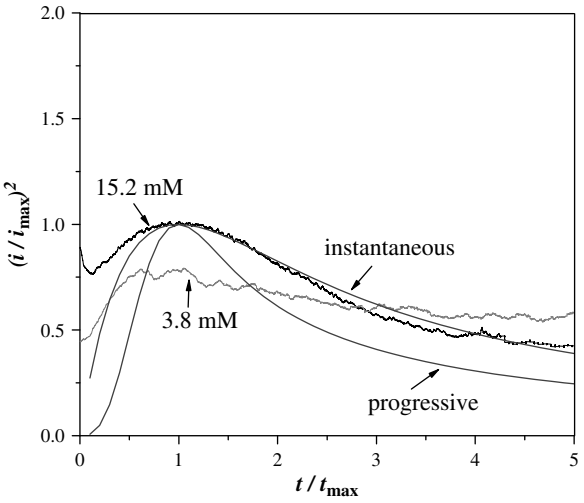


**Fig. 7.** Comparison of the dimensionless experimental data derived from the current transients for 15.2 mM and 3.8 mM Au(I) with the theoretical curves for instantaneous and progressive nucleation.

the one reported for thiosulfate $7.01 \times 10^{-6}\ cm^2\ s^{-1}$ [19]. The kinetic analysis delivers more; it is also possible to gain information regarding the number of active sites $N$ on the electrode from the equation:

$$i_{max} = 0.6382zFDc(kN)^{1/2} \quad (5)$$

the constant $k$ is related to the density and molar mass of the nuclei according to:

$$k = (8\pi cM/\rho)^{1/2} \quad (6)$$

from these relationships, the density of active sites on the sample was calculated as $5.5 \times 10^8$ sites $cm^{-2}$.

The experimental data obtained for the transients corresponding to 3.8 mM Au(I) concentrations showed an initial increase before dropping to the diffusion limited domain described by Cottrell. This behaviour can be correlated to the growth of gold hemispheres on the tungsten fibres as described by Nagy et al. [20,21]. The current increase at short times is due to the growth of individual deposits, whereas the maximum can be explained by the overlapping of the diffusion zones for each growing hemisphere.

The poor agreement observed for the experimental data with the theoretical models described in the literature suggests that the total recorded current could be the sum of the current due to more than one process, namely the oxidation of the remaining W fibres to form oxides of different nature. The current due to this process would not be separated from the overall recorded current, and thus could yield to an erroneous analysis. However, it is worth noting that despite this inconvenience, it is still possible to obtain kinetic analysis of the system under certain experimental conditions. Even in the cases when the nucleation process could not be accurately determined, the electrodeposition process often resulted in the formation of small structures inside the pores and rarely protruding from the edges. Examples of such structures are shown in Fig. 8, where spherical gold deposits are observed inside the W pore, as corroborated by EDX analysis. Further deposits are also observed outside the pore, with a rougher and more irregular surface. These deposits are the result of salt precipitates from the electrolyte during the deposition process. A clear proof on the nature of the latter ones could not be performed till now and will be the object of further studies in which these precipitates will be directly harvested by means of nano tweezers in a SEM. Further experiments should concentrate on the formation of smoother

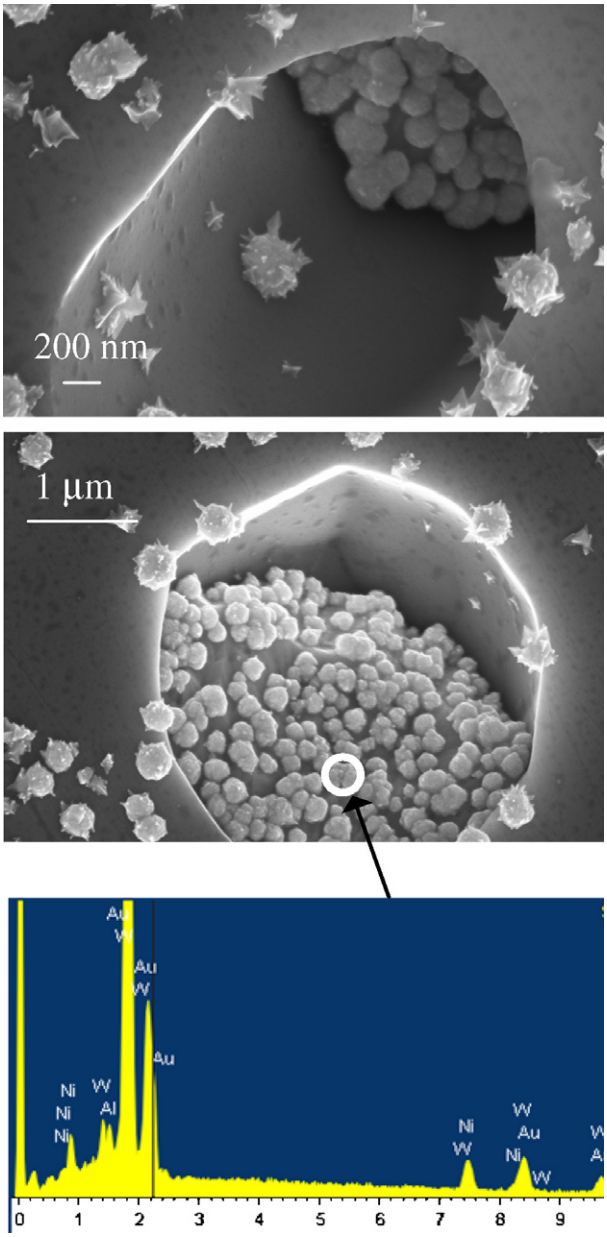


**Fig. 8.** Examples of gold deposits obtained in NiAl–W eutectics after deposition for 30 min at −0.7 V (vs. counter) from a solution containing 7.6 mM Au(I). The EDX spectrum on a single nucleus on the nanowire inside the pore shows that it is a gold deposit. See text for further details.

deposits by application of less negative overpotentials for the electrodeposition of Au(I) ions, or the use of alternative electrolyte solutions [22–25]. Due to the passivation of the matrix, only the wires and later the gold deposits remain electrochemically active which gives this approach an inherent advantage over an alternative route in which the gold electrodes are directly produced as the minor phase of a directionally transformed eutectoid system [26,27].

## 4. Conclusion

The electrodeposition of gold into the pores created in NiAl–W eutectic alloys by selective oxidation of the W fibres has been optimised in terms of the pre-passivation potential, deposition potential, concentration of Au(I) ions, and duration of the process. It was found that the oxidation of the W fibres must be run at a potential sufficiently anodic to enable the growth of a thick oxide film on the NiAl matrix, thus preventing this phase from remaining electrochemically active. The deposited gold hemispheres had a radius that increased with the duration of the deposition process. The density of hemispheres increased initially but reached a fairly constant value after a certain time, due to the overlapping of the deposits. Kinetic studies into the nucleation and growth mechanisms of the gold structures from solutions containing different Au(I) concentrations suggested that the process is mainly governed by instantaneous nucleation followed by diffusion controlled growth of the nuclei for a Au(I) concentration of 15.2 mM. Lower amounts of the Au(I) ions resulted in either mixed phenomena, or processes compiling with the Cottrell behaviour. The difficulties encountered for the kinetic investigations may result from the complex nature of the studied system, in which the oxidation of the W fibres could interfere with the electrodeposition process. Nevertheless, the data reported so far throws some light in the mechanisms of oxidation and electrodeposition on complex substrates. For diluted concentrations of the ions, the obtained structures form a thin film on the W fibres, thus creating an array of gold nanoelectrodes (100 nm) on the passive NiAl matrix. The nanoelectrode array could have applications in the sensor technology field.

## Acknowledgements

The financial support of the Deutsche-Forschungs-Gemeinschaft through the projects *Production of Nanowire Arrays through Directional Solidification and their Application*, HA3118/4-1 and *Application of Directionally Solidified Nanowire Arrays*, HA 3118/4-2 within the DFG Priority Program 1165 *Nanowires and Nanotubes-from Controlled Synthesis to Function* is gratefully acknowledged. The authors are also grateful to Dr. Srdjan Milenkovic for the solidification of the employed eutectics.

## References

[1] F. Keller, M.S. Hunter, D.L. Robinson, J. Electrochem. Soc. 100 (1953) 411–413.
[2] M.S. Sander, L.S. Tan, Adv. Funct. Mater. 13 (2003) 393–397.
[3] M. Gillet, K. Masek, C. Lemire, Thin Solid Films 444 (2003) 9–16.
[4] K. Kim, M. Kim, S.M. Cho, Mater. Chem. Phys. 96 (2006) 278–282.
[5] K.R. Pirota, D. Navas, M. Hernandez-Velez, K. Nielsch, M. Vazquez, J. Alloy Compd. 369 (2004) 18–26.
[6] A.W. Hassel, B. Bello Rodriguez, S. Milenkovic, A. Schneider, Electrochim. Acta 50 (2005) 3033–3039.
[7] A.W. Hassel, B. Bello Rodriguez, S. Milenkovic, A. Schneider, Electrochim. Acta 51 (2005) 795–801.
[8] A.W. Hassel, A.J. Smith, S. Milenkovic, Electrochim. Acta 52 (2006) 1799–1804.
[9] F.H. Jones, R.G. Egdell, A. Brown, F.R. Wondre, Surf. Sci. 374 (1997) 80–94.
[10] D.W. Letcher, T.J. Cardwell, R.J. Magee, J. Electroanal. Chem. 25 (1970) 473–479.
[11] B. Bello Rodriguez, A.W. Hassel, J. Electrochem. Soc. 153 (2006) C33–C36.
[12] B. Bello Rodriguez, A.W. Hassel, J. Electrochem. Soc. 155 (2008) K31–K37.
[13] T. Osaka, Y. Okinaka, J. Sasano, M. Kato, Sci. Technol. Adv. Mater. 7 (2006) 425–437.
[14] D. Dobrev, J. Vetter, N. Angert, R. Neumann, Electrochim. Acta 45 (2000) 3117–3125.
[15] M. Pourbaix, Atlas of Electrochemical Equilibria in Aqueous Solutions, National Association of Corrosion Engineers, Texas, USA, 1974.
[16] G.S. Kelsey, J. Electrochem. Soc. 124 (1977) 814–819.
[17] B. Scharifker, G. Hills, Electrochim. Acta 28 (1983) 879–889.
[18] G. Gunawardena, G.J. Hills, I. Montenegro, B. Scharifker, J. Electroanal. Chem. 138 (1982) 225–239.
[19] A.M. Sullivan, P.A. Kohl, J. Electrochem. Soc. 144 (1997) 1686–1690.
[20] G. Nagy, Y. Sugimoto, G. Denuault, J. Electroanal. Chem. 433 (1997) 167–173.
[21] G. Nagy, G. Denuault, J. Electroanal. Chem. 433 (1997) 175–180.
[22] Y. Okinaka, M. Hoshino, Gold Bull. 31 (1998) 3–13.
[23] Y. Okinaka, Gold Bull. 33 (2000) 117–127.
[24] M. Kato, Y. Okinaka, Gold Bull. 37 (2004) 37–44.
[25] T.A. Green, Gold Bull. 40 (2007) 105–114.
[26] S. Milenkovic, A. Schneider, A.W. Hassel, Gold Bull. 39 (2006) 185–191.
[27] Y. Chen, S. Milenkovic, A.W. Hassel, Nano Lett. 8 (2008) 737–742.